PNAS

Supplementary Information for

eIF2Bδ blocks the integrated stress response, maintains eIF2B activity and cancer metastasis by overexpression in breast cancer stem cells

Malavika Gupta[1,‡], Beth A. Walters[1,§], Olga Katsara[1], Karol Grenados-Blanco[1], Phillip A. Geter[1,†] and Robert J. Schneider[1,2,*]

[1] Department of Microbiology, NYU Grossman School of Medicine, New York, NY 10016 USA
[2] NYU Perlmutter Cancer Center, NYU Grossman School of Medicine, New York, NY 10016 USA
[§] Present address: Ultragenyx Pharmaceuticals, 60 Leveroni Court, Novato, CA 94949
[†] Wunderman Thompson Health, 3 World Trade Center, New York, NY 10007
[‡] Carecam International, Inc, Fairfield, NJ 07004

***Corresponding author:** Robert J. Schneider

Email: Robert.schneider@nyumc.org

This PDF file includes:

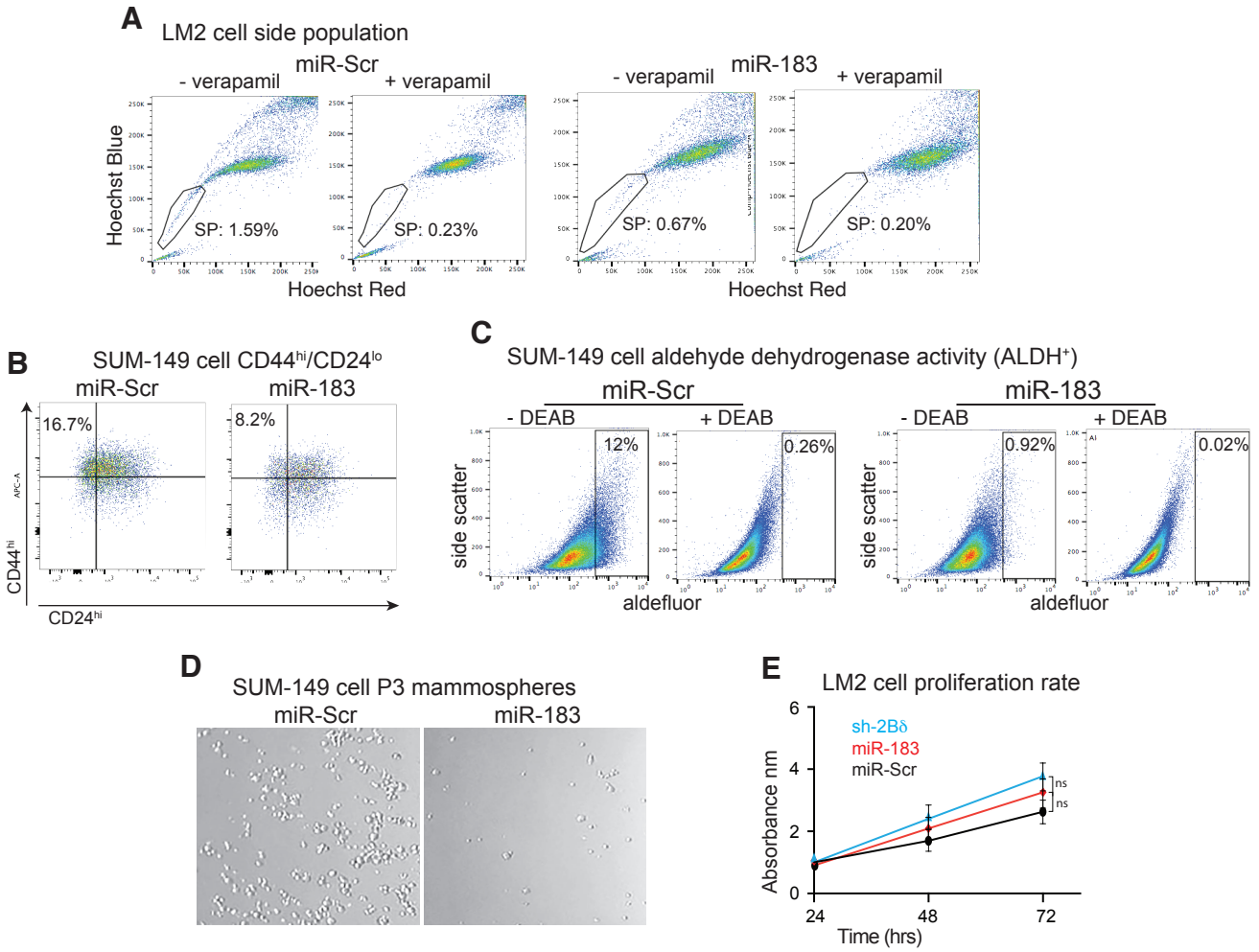

Fig. S1. Reduction in eIF2Bδ decreases breast CSCs and mammosphere formation but does not significantly alter cell proliferation rate. (*A*) Gating strategy for determination of CSCs by side population. Representative side population results for LM2 cells constitutively expressing non-silencing control miR-Scr or miR-183. (*B*) Gating strategy for determination of CSCs by $CD44^{hi}/CD24^{lo}$. Representative $CD44^{hi}/CD24^{lo}$ results for SUM-149 cells constitutively expressing non-silencing control miR-Scr or miR-183. (*C*) Gating strategy for determination of CSCs by $ALDH^{+}$. Representative $ALDH^{+}$ results for SUM-149 cells constitutively expressing non-silencing control miR-Scr or miR-183. (*D*) Representative light microscope images of passage 3 (P3) mammospheres at 5x magnification for SUM-149 cells expressing non-silencing control miR-Scr or miR-183 cells seeded on ultra-low attachment plates. Equal numbers of cells used for seeding studies. (*E*) Proliferation rates were determined using equal numbers of LM2 cells expressing miR-Scr, miR-183 or sh-2Bδ. Relative absorbance at 570 nm for MTT uptake was plotted normalized to the 24 h time point for each cell line. Data are means ± SEM determined not significant (ns) by two-tailed unpaired t-test from 3 independent studies.

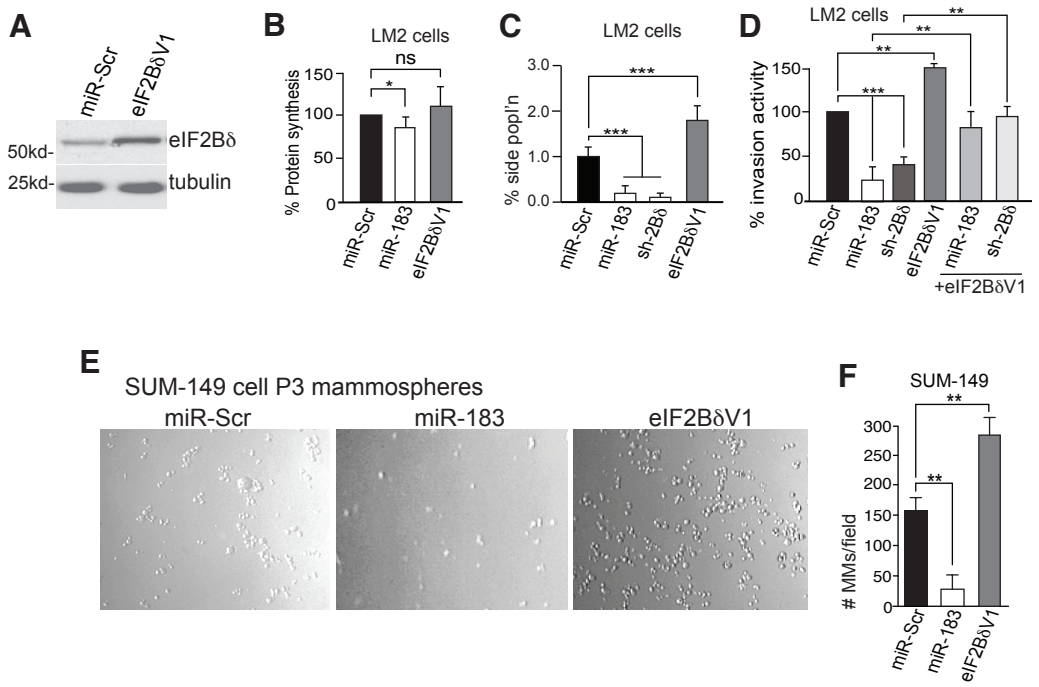

Fig. S2. Effect of eIF2Bδ expression level on breast cancer cell protein synthesis, CSC number and function. (*A*) LM2 cells were stably transfected with non-silencing miR-Scr or a plasmid expressing eIF2BδV1. Equal amounts of protein lysates were subjected to immunoblot for eIF2Bδ or invariant tubulin. Representative immunoblot of two studies. (*B*) Protein synthesis rate determined in LM2 cells expressing control miR-Scr, miR-183, or a plasmid expressing eIF2BδV1. Results of 3 independent studies. (*C*) Percent side population representative of CSCs in cells stably expressing miR-Scr, miR-183, sh-2Bδ or eIF2BδV1 mRNA. (*D*) Percent Matrigel transwell invasion activity of LM2 cells stably expressing non-silencing control miR-Scr, miR-183, sh-2Bδ, and/or eIF2BδV1 mRNA. Results of 3 independent studies. (*E*) Representative light microscope images of passage 3 (P3) mammospheres at 5x magnification for SUM-149 cells expressing non-silencing control miR-Scr, miR-183 or eIF2BδV1 mRNA. Equal numbers of cells were seeded on ultra-low attachment plates. (*F*) Mammospheres as shown in (E) were quantified, scoring only those that contained ≥30 cells, from 5 visual fields at 5x magnification chosen at random. ns, not significant, *P<0.05, **P<0.01, ***P<0.001 ± SEM by two-tailed unpaired t-test from 3 independent studies.

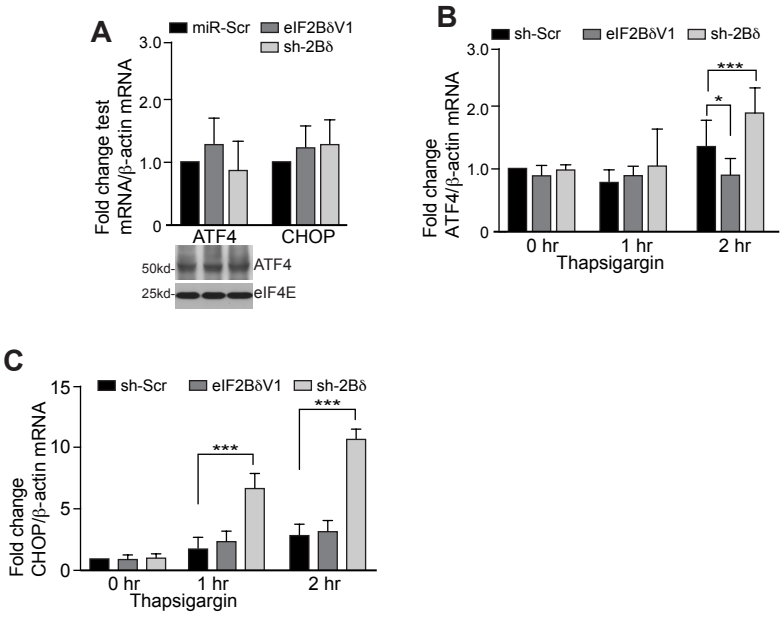

Fig. S3. Increased expression of eIF2Bδ represses the ISR in breast cancer cells. (*A*) Relative ATF and CHOP mRNA levels determined by qRT-PCR in LM2 cells expressing miR-Scr, sh-2Bδ or eIF2BδV1 mRNA normalized to β-actin. No significant differences. Immunoblot, ATF4 protein from equal amounts of protein lysates. n=3. (*B*) ATF4 mRNA normalized to β-actin quantified by qRT-PCR from LM2 cells. n=3. (*C*) CHOP mRNA normalized to β-actin quantified by qRT-PCR from LM2 cells. n=3. *P<0.05, ***P<0.001 with SEM by two-tailed unpaired t-test from 3 independent trials.

Table S1. Description of the cell lines used for the isolation of cancer stem cells and extraction of miRNAs for analysis.

Cell line	Genotype	Adherent cells	P2 Mammosphere	Aldefluor Positive	$CD44^{hi}CD24^{lo}$	Side popl'n
HME-t7ert	Immortalized; non-tumor forming	Yes	No (does not form)	Yes	Yes	No
CRL1902/UACC-893	Stage 3 [1] IDC, $p53^+$, $Her2^-$ ER^-/PR^-	Yes	Yes	Yes	Yes	Yes
CRL 2315/HCC70	Stage 3 IDC, $p53^+$, $Her2^-$ ER^-/PR^-	Yes	Yes	Yes	No	Yes
LM2	Stage 4 IDC; $p53^-$, ER^- PR^- $Her2^-$derived from MB231 metastasis to lung	Yes	Yes	[3] No	[4] No	Yes
SUM 149	IBC; $Her2/neu^-$, ER^- PR^-	Yes	Yes	Yes	Yes	Yes
MCF10A	Non-tumor forming	Yes	Yes	Yes	Yes	Yes
MCF7	$Her2/neu^-$, ER^+ PR^+	Yes	Yes	[5] Yes	[5] Yes	[5] Yes
HTB-20/BT-474	Stage 4 IDC grade 3, $p53^+$, ER^+ PR^-	Yes	Yes	Yes	Yes	Yes
MB-231	Stage 4 IDC; pleural lung effusion, $p53^-$ ER^- PR^-Her2^-	Yes	Yes	Yes	No	Yes

[1] IDC (invasive ductal carcinoma)

[2] IBC (inflammatory breast cancer)

[3] Expresses overlapping GFP reporter

[4] Expresses 99% $CD44^{hi}CD24^{lo}$

[5] Expresses but low levels

Table S2. Top differentially expressed miRNAs identified from the miRNA qPCR array.

miRNA	Fold change (log_2)	Target genes
hsa-miR-500-4395539	-5.753494933	ING1 (4)
hsa-miR-10b-4395329	-5.504056729	CADM1, MICB, Apaf-1, HOXB3, NF1, HOXD10, TBX5, Tiam1, Vimentin, Syndecan-1, SFRS1, KFL4 (5)
hsa-miR-502-3p-4395194	-5.269260195	PRNP, PRKX, MAPK1, PRKACB, TJP1, SEMA3C (6)
hsa-miR-501-3p-4395546	-4.63055966	CDK6, MYBL2, TOMM20, CLIC4, DIAPH1 (7)
hsa-miR-32-4395220	-4.500828993	PTEN (8) BTG2 (9)
hsa-miR-96-4373372	-4.151608639	PTPN9 (10)
hsa-miR-579-4395509	-4.118801763	ZFR (11) GSK3B, NRAS, TCF4, APC, PI3K3CB, EGFR, CTNNA1, PDK1, PIK3KI (12)
hsa-miR-34c-5p-4373036	-3.946471773	NOTCH1 (13) MAPT (8) BMF (14)
hsa-miR-139-3p-4395424	-3.773593638	RAB1A (15) NOB1 (16)
hsa-miR-183-4395380	-3.723119108	FOXO1 (17) ITGB1, UFM1, IDH2 (18) VIL2 (ezrin) (19)
hsa-miR-21-4373090	2.368323733	JAG1, WNT1 (20) SPRY1, PTEN (21)
hsa-miR-363-4378090	2.386401745	PTEN, BIM (22) PDPN (23)
hsa-miR-222-4395387	2.509625447	PUMA, P27 (KIP1), P57 (24) NOTCH3 (25)
hsa-miR-29a-4395223	2.54490064	CDK2, CDK4, CDK6, MMP13, ITGB1, MMP2, TRIM68, VEGF (26)
hsa-miR-342-3p-4395371	2.642099514	Bcl2 (27) ID4 (28) ATF3 (29)
hsa-miR-106a-4395280	2.649219262	IL-10 (30)
hsa-miR-218-4373081	2.662012297	SERBP1 (PMID: 28369267), IL-6, STAT3 (31)
hsa-miR-106b-4373155	2.754469049	NR2FS-AS1, PLEKHO2 (32)
hsa-miR-30c-4373060	2.999224996	NOV/CCN3 (33)
hsa-miR-24-4373072	3.174586802	Jab1/CSV5 (34), Prdx6 (35), SOX7 (36)

Supplemental Materials and Methods

Cells and cell culture. Human mammary epithelial (HME) cells immortalized by tert transformation (HME-tert cells) were provided by Robert Weinberg (1) and cultured in Mammary Epithelial Growth Medium (MEGM BulletKit, Lonza). MDA-MB-231 LM2 variant cells and 293FT packaging cells were obtained from Cellosaurus. Cell lines were cultured at 37 °C in 5% CO_2 using media and supplements individualized for each cell line. CRL1902, CRL2315, BT-474, MCF10A, MCF7 and MB-231 cells were obtained from the American Type Culture Collection (ATCC, Manassas, VA, USA). LM2, CRL1902, CRL2315, MCF10A, MCF7 and MB-231 cells were cultured in DMEM with 2 mM Glutamine, 1 mM sodium pyruvate, gentamycin, and 10% FBS. SUM149 cells were cultured in Hams F12 medium with 5% FBS, 40 μg/mL gentamycin, 0.5 μg/mL amphotericin, 5 μg/mL insulin, and 1 μg/mL hydrocortisone. BT-474 cells were cultured in DMEM with 2 mM Glutamine, 1X NCTC135, 0.165 g/mL oxaloacetic acid, 0.01 mg/mL insulin, 10 mM HEPES, pH7.0, 1 mM sodium pyruvate, non-essential amino acids, 0.22 g/L sodium bicarbonate, 30 ng/mL EGF, 10% FGF, and gentamycin. Generation and characterization of cells with stable inducible silencing shRNAs or cDNAs are described below. All cell lines were authenticated by short tandem repeat profiling and routinely checked for mycoplasma contamination.

Vectors and cloning. The miR183 sequence (Key Resources Table) was annealed to its complementary sequence to generate a duplex that was cloned into pLKO-Tet-On or pLKO constitutive vectors, using AgeI and EcoRI linkers. Sh-2Bδ, Flag-eIF2Bδ variant 1 was provided by Dr. Martin (2) (NYU Langone School of Medicine). miRZIP scrambled and miRZIP-183 constructs were gifts from Drs. Hanniford and Hernando (NYU Langone School of Medicine) (3).

Cell viability-proliferation assays. The 3-(4,5-dimethylthiazol-2-yl)-2,5-diphenyltetrazolium bromide (MTT) assay was performed using the CellTiter 96 Non-Radioactive Cell Proliferation Assay according to manufacturer instructions (Promega, Madison, WI, USA). Cells were seeded onto 96-well plates at an optimal density of 5×10^3 cells per well and incubated overnight at 37 °C. During a period of 1 to 3 d cells were treated with Dox (1 μg/mL for LM2 cells, 0.5 μg/mL for SUM-149 cells) to measure the effect of gene silencing on cell proliferation. Cells were treated with 15 μL MTT dye and cultures were re-incubated for an additional 4 h. Following removal of the supernatant, 100 μL of the Solubilization Solution/Stop Mix was added to each well to completely dissolve the crystals and absorbance was measured at 570 nm using a 96-well plate reader.

Mammosphere formation. For mammosphere formation, single cell suspensions of growing cells were resuspended in 4 mL of 3D Tumorsphere Media XF (Millipore Sigma) at a density of 1,000 cells/mL and plated in 6-well low-adherence tissue culture plates (Nunc, Millipore Sigma) to prevent cell attachment. After 4-7 d in culture, mammospheres were collected by gentle centrifugation (200 x g), washed by gentle centrifugation twice in

cold 1x PBS, dissociated enzymatically (5 min at room temperature in 1:1 trypsin/TumorSphere media), trypsin neutralized with Trypsin Neutralization solution (Sigma) and mechanically disrupted by passing through a 25G needle (6 strokes). Single cells were re-plated at a density as above for subsequent passage 1 and passage 2. Second passage mammospheres that are highly enriched in cancer stem cell populations were used for isolation of miRs and other studies.

Matrigel Invasion assay. Invasion assays were performed using Corning BioCoat Matrigel Invasion Chamber with Corning Matrigel Matrix (Thermo Fisher Scientific) per manufacturer instructions. After Dox treatment as described above, a suspension of 1 x 10^5 cells in 500 µL of serum-free media were added to the upper chambers, and 10% FBS added to the lower chambers. After 18-24 h at 37 °C, 5% CO_2, cells that had migrated through the membrane were fixed with methanol and stained with 1% of crystal violet. Invading cells per field were scored and performed in triplicate (n=12) using a ZEISS Axio light microscope (100× magnification) and ZEISS software (Carl Zeiss Meditec, Inc., San Diego, CA, USA). All experiments were performed in the presence of hydroxyurea at 1 µM as an inhibitor of proliferation.

Metabolic protein synthesis rate labeling with [^{35}S]-methionine. Cells were pulse-labeled for 120 min with 50 µCi of a [^{35}S]-methionine and cysteine mix per ml (Easytag express protein labeling mix; PerkinElmer) in DMEM without methionine and cysteine and with 2% dialyzed FBS (HyClone). Cells were lysed in RIPA lysis buffer and assayed by trichloroacetic acid (TCA) precipitation onto GF/C filters and liquid scintillation counting.

Immunoblot Analysis and antibodies. Total protein was extracted by RIPA buffer extraction (150 mM NaCl, 50 mM Tris pH 8.0, 1% NP-40) containing Halt Phosphatase Inhibitor Cocktail (Thermo Fisher Scientific), Pierce Protease Inhibitor Tablet (Thermo Fisher Scientific), clarified by microfuge centrifugation at 4°C, and protein concentration determined using the Pierce BCA Protein Assay Kit (Thermo Fisher Scientific). Equal amounts of denatured protein lysates were resolved by SDS-PAGE, transferred to polyvinylidene difluoride (PVDF) membrane, blocked with 5% Bovine Serum Albumin (BSA) for 1 h and incubated at 4°C overnight with primary antibodies at 1:1000 dilution against respective proteins. Proteins were visualized using ECL and anti-Rabbit IgG or anti-Mouse IgG, Horseradish Peroxidase (HRP) linked whole antibody (Catalog no., NA934V and NA931V, respectively; GE Healthcare Bio-sciences Corp., Piscataway, NJ, USA) diluted to 1:10,000 in 1x TBS-T for 1 h at room temperature. Results were quantified using ImageJ software.

eIF2B GEF activity. eIF2B GEF activity was carried out as described (38). Briefly, 1x10^6 LM2 cells expressing control vector, miR-183, sh-2Bδ or eIF2BδV1 were lysed in 100 µL of 45 mM HEPES, pH 7.4, 0.375 mM $Mg(OAc)_2$, 0.075 mM EDTA, 95 mM $K(OAc)_2$, 10% glycerol, 0.5% Triton X-100, and protease inhibitors at 4°C,. Lysates were clarified by microfuge centrifugation at 10,000 x g for 10 min at 4°C, and supernatants kept at 4˚C and used for GEF activity determination. Protein concentration was determined on aliquots of

supernatant for each sample. 100 μL of supernatant was combined with 120 μl of 4˚C reaction buffer: 50 mM MOPS, pH 7.4, 100 mM KCl, 1 mM DTT, 2 mM $Mg(OAc)_2$, 225 mM GDP, 0.2 mg/ml BSA, and warmed to 30˚C. The reaction was initiated by addition of 3 μg eIF2-[^{3}H]GDP complex to each tube (a kind gift of S. Kimball, Penn State University) was added to the tube and the contents were mixed. Aliquots of 30 μl were removed every 2 min until depleted to 2.5 ml of ice-cold 50 mM MOPS, pH 7.4, 2 mM $Mg(OAc)_2$, 100 mM KCl, 1 mM DTT, mixed and filtered through nitrocellulose filters. Filters were dried and quantified [^{3}H]GDP bound to the filters by liquid scintillation counting in FiltronXM scintillation cocktail (Life Science Products), normalized to mixtures without added eIF2 and protein content. Exchange rates of [^{3}H]GDP for non-radioactive GDP were calculated by linear regression analysis and repeated 3 times.

eIF2Bδ-eIF2 immunoprecipitation studies. LM2 cells were transiently transfected with an expression plasmid encoding eIF2BδV1-Flag, 24 h later treated with 30 μM thapsigargin or vehicle for 2 h, and cell lysates subjected to Flag immunoprecipitation. Immunoprecipitates were resolved by SDS-PAGE and immunoblotted for eIF2Bδ, eIF2α, eIF2α-Ser51P, eIF2β and eIF2γ.

eIF2B protein miR and short hairpin RNA (shRNA) silencing. Lentiviruses were produced by transient transfection of human embryonic kidney (HEK) 293FT cells with individual lentiviral vectors containing the pLKO-Tet-On or pLKO constitutive vectors with packaging plasmids pMD2G and psPAX2 (Addgene, Cambridge, MA, USA) using Lipofectamine 2000 (Promega, Madison, WI, USA). Supernatants containing viral particles were collected 48 h post-transfection, filtered through 0.45 μm filters and viral particles concentrated using the PEG-itTM Virus Precipitation Solution Kit (System Biosciences, Mountain View, CA, USA). Cloning of the shRNA cassette sequences for eIF2Bδ and non-silencing sequence control Nsi (5'-AATTCTCCGAACGTGTCACGT-3') were previously described (34). Cells were infected with viral particles, selected with puromycin (1 μg/ml). The lentiviral vectors used for miR-183, miR-Scr, and sh-eIF2Bδ contain a constitutively expressed transcript encoding the puromycin resistance gene. Cells were treated with 0.1 to 2 μg/ml of Dox and FACs isolated gating on GFP for ALDH assays.

Flow cytometry of CD44^{hi}/24^{lo} population. For cell sorting, typically 2X10^6 cells were incubated with anti-human CD24 and anti-human CD44 for 30 mins on ice. After the incubation, cells were washed 2X with a solution of 2% FBS/PBS and resuspended at 1X10^6 cells/mL in 2% FBS/PBS. Cells were sorted using FACSARIA II cell sorter. For cell analysis, 2X10^5 cells were used for the labeling reaction and analyzed using the LSR II UV analyzer. Antibody concentrations were titrated and optimized before sorts and analyses.

Side population flow cytometry. 500,000 cells were stained with bisBenzimide H 33342 trihydrochloride, and half of the sample was co-treated with 50 μM verapamil hydrochloride. Incubations were carried out at 37°C for 30 min after which cells were washed 2X with ice cold 2% FBS/PBS, resuspended in ice cold 2% FBS/PBS and analyzed using an LSR II UV analyzer.

Tumor lysis and extract preparation. Tumors were homogenized using a pellet pestle in RIPA lysis buffer which consisted of 1% Triton X-100, 1% sodium deoxycholate, 0.1% SDS, 150 mM NaCl, 50 mM Tris, pH 7.4, 2 mM Na_3VO_4, 25 mM β-glycerophosphate, 15 mM NaF, and complete protease inhibitor mix (Roche). Protein concentrations in the lysates of cells lysed in RIPA lysis buffer were determined using a DC protein assay kit (Bio-Rad).

Sucrose density gradient analysis of eIF2B complexes. Sucrose gradient studies were conducted as previously described (36). Briefly, LM2 cells were collected and washed with ice-cold PBS and then lysed in lysis buffer (50 mM Tris pH=7.5, 400 mM KCl, 4 mM $Mg(OAc)_2$, 0.5% Triton X-100, and protease inhibitors). Lysates were clarified and ribosomes were removed by pelleting under high-speed centrifugation at 100,000xg for 30 mins at 4°C. Supernatants were layered on top of 5-20% sucrose gradients and centrifuged for 14 h at 40,000 rpm at 4°C using a SW55 rotor. Equal fractions were collected, proteins chloroform-methanol precipitated and resolved by SDA-PAGE.

RESOURCES and ANTIBODIES TABLE

REAGENT or RESOURCE	SOURCE	IDENTIFIER/RRID
Antibodies		
Rabbit polyclonal anti-human/mouse β-actin antibody	Cell Signaling Technology	Cat# 4967/ RRID:AB_330288
Rabbit monoclonal anti-human/mouse GAPDH antibody	Cell Signaling Technology	Cat# 2118S/ RRID:AB_561053
Rabbit monoclonal anti-human/mouse eIF2Bα	Abcam	Cat# ab40744
Rabbit monoclonal anti-human/mouse eIF2Bβ	Abcam	Cat# ab133848
Rabbit monoclonal anti-human/mouse eIF2Bγ	Abcam	Cat# ab135351
Rabbit monoclonal anti-human/mouse eIF2Bδ	Abcam	Cat# ab124468
Rabbit monoclonal anti-human/mouse eIF2Bε	Abcam	Cat# ab155665
Rabbit polyclonal anti-human/mouse eEF2	Cell Signaling Tech.	Cat# 2332S
Rabbit polyclonal anti-human/mouse eEF2α-P	Cell Signaling Tech.	Cat# 9721S
Mouse monoclonal anti-human/mouse eIF4E	BD Biosciences	Cat# 610270
Mouse monoclonal anti-FLAG	Sigma-Aldrich	Cat# F3165
Mouse monoclonal anti-human CD44	BD Biosciences	Cat# 559942
Mouse monoclonal anti-human CD24	BD Biosciences	Cat# 555428
Rabbit polyclonal anti-mouse/human eIF2α	Proteintech	Cat# 11170-1-AP
Rabbit polyclonal anti-mouse/human eIF2α Ser51P	Proteintech	Cat# 28740-1-AP
Rabbit monoclonal anti-mouse/human eIF2γ	Abcam	Cat# ab33207
Bacterial and virus strains		
Chemicals, peptides, and recombinant proteins		
human bFGF	StemCell Technologies	Cat# 78003
human EGF	StemCell Technologies	Cat#78006
Oligofectamine	ThermoFisher	Cat#12252011
Verapamil hydrochloride	Sigma-Aldrich	Cat# 152-11-4
DAPI Fluorescent Stain	Cell Biolabs, Inc.	Cat# 112002
D-luciferin	Perkin-Elmer	Cat# 122799
Halt™ Phosphatase Inhibitor Cocktail	ThermoFisher	
Pierce Protease Inhibitor Tablet	ThermoFisher	
Lipofectamine™ 2000	Promega	Cat# 11668019
PEG-itTM Virus Precipitation Solution Kit	System Biosciences	Cat# LV825A-1
bisBenzimide H 33342 trihydrochloride	Sigma-Aldrich	Cat# 23491-52-3
Mammary Epithelial Growth Medium (MEGM), BulletKit	Lonza	Cat# CC3150
PromoCell 3D TumorSphere media XF	Millipore Sigma	Cat# C28070
Critical commercial assays		
High-Capacity cDNA Reverse Transcription Kit	ThermoFisher	Cat# 4368814
Maxima SYBR Green qPCR Master Mix	Bio-Rad Laboratories	Cat# K1070
FITC Annexin V apoptosis kit	BD Biosciences	Cat# 556547
Pierce BCA Protein Assay Kit	ThermoFisher	Cat# 23228
Aldefluor Kit	Stem Cell Technologies	Cat# 01700
Corning BioCoat Matrigel Invasion Chamber	Thermo Fisher	Cat# 08-774-122
CellTiter 96® Non-Radioactive Cell Proliferation MTT Assay	Promega	Cat# G9241
miRvana miRNA Isolation kit	ThermoFisher	Cat# AM1560

TaqMan qPCR arrays	ThermoFisher	Cat# 4398965
PEG-itTM Virus Precipitation Solution Kit	System Biosciences	Cat# LV810A-1
TaqMan Advanced miRNA assay kit	ThermoFisher	Cat# A25576
TaqMan Advanced miRNA cDNA kit	ThermoFisher	Cat# A28007
TaqMan Fast Advanced synthesis master mix	ThermoFisher	Cat# A44456
Nunc 6 well low adherence culture plates	Millipore Sigma	Cat# 2721050
Deposited data		
Experimental models: Cell lines		
Human: MDA-MB-231 cells	ATCC	Cat# CRM-HTB-26/ RRID:CVCL_006
Human: MDA-MB-231 LM2 variant cells	Cellosaurus	MDA231-LM2-4175 (RRID:CVCL_5998)
Human: HEK 293FT	Cellosaurus	RRID:CVCL_6911
Human: CRL1902/UACC-893 cells	ATCC	Cat# CRL-1902
Human: CRL2315/HCC70 cells	ATCC	Cat# CRL-2315
Human: SUM149 cells	Cellosaurus	Cat# CVCL_3422
Human: MCF10A /CRL-10317 cells	ATCC	Cat# CRL-10317
Human: HTB20/BT474 cells	ATCC	Cat# BT-474
Human: HME-tert cells	MIT	
Human: MCF7/HTB-22 cells	ATCC	Cat # HTB-22
Experimental models: Organisms/strains		
NOD SCIDγ mice	Jackson Labs	Cat# 005557
Oligonucleotides (5' to 3' shown)		
miR-183: 5'ccgcagagtgtgactcctgttctgtgtatggcactggtagaattcactgtgaacagtct cagtcagtgaattaccgaagggccataaacagagcagagacagatccacga3'	This paper	N/A
Non-silencing (Nsi) control shRNA 5'-AATTCTCCGAACGTGTCACGT-3'	This paper	N/A
Recombinant DNA		
pMD2G	Addgene	Cat# 12259
pTRIPZ	Addgene	Cat# 127696
psPAX2	Addgene	Cat# 12260
miRZIP-183	{Segura, 2017 #37}	N/A
miRZIP scrambled	{Segura, 2017 #37}	N/A
Software and algorithms		
GraphPad Prism 8 & 9 software	GraphPad	https://www.graphpad.com
FlowJo	FLowJo	https://www.flowjo.com
EVOS™ FL Imaging System	ThermoFisher	https://www.thermofisher.com/us/en/home/technical-resources/software-downloads/evos-fl-cell-imaging-system.html

SI References

1. B. Elenbaas *et al.*, Human breast cancer cells generated by oncogenic transformation of primary mammary epithelial cells. *Genes Dev* **15**, 50-65 (2001).
2. L. Martin, S. R. Kimball, L. B. Gardner, Regulation of the unfolded protein response by eif2Bdelta isoforms. *The Journal of biological chemistry* **285**, 31944-31953 (2010).
3. M. F. Segura *et al.*, Kruppel-like factor 4 (KLF4) regulates the miR-183~96~182 cluster under physiologic and pathologic conditions. *Oncotarget* **8**, 26298-26311 (2017).
4. M. Jiang, L. Y. Zhou, N. Xu, Q. An, Down-regulation of miR-500 Nand miR-628 suppress non-small cell lung cancer proliferation, migration and invasion by targeting ING1. *Biomed Pharmacother* **108**, 1628-1639 (2018).
5. P. Sheedy, Z. Medarova, The fundamental role of miR-10b in metastatic cancer. *Am J Cancer Res* **8**, 1674-1688 (2018).
6. M. Grasso *et al.*, Plasma microRNA profiling distinguishes patients with frontotemporal dementia from healthy subjects. *Neurobiol Aging* **84** (2019).
7. N. Hara *et al.*, Serum microRNA miR-501-3p as a potential biomarker related to the progression of Alzheimer's disease. *Acta Neuropathol Com* **5** (2017).
8. W. Y. Wu *et al.*, MicroRNA-32 (miR-32) regulates phosphatase and tensin homologue (PTEN) expression and promotes growth, migration, and invasion in colorectal carcinoma cells. *Molecular Cancer* **12** (2013).
9. S. E. Jalava *et al.*, Androgen-regulated miR-32 targets BTG2 and is overexpressed in castration-resistant prostate cancer. *Oncogene* **31**, 4460-4471 (2012).
10. Y. T. Hong *et al.*, miR-96 promotes cell proliferation, migration and invasion by targeting PTPN9 in breast cancer. *Sci Rep-Uk* **6** (2016).
11. L. C. Hinske *et al.*, Alternative Polyadenylation Allows Differential Negative Feedback of Human miRNA miR-579 on Its Host Gene ZFR. *PloS one* **10** (2015).
12. Widodo, M. S. Djati, M. Rifa'i, Role of MicroRNAs in carcinogenesis that potential for biomarker of endometrial cancer. *Ann Med Surg* **7**, 9-13 (2016).
13. H. L. Wei *et al.*, miR-34c-5p targets Notch1 and suppresses the metastasis and invasion of cervical cancer. *Mol Med Rep* **23** (2021).
14. S. Catuogno *et al.*, miR-34c may protect lung cancer cells from paclitaxel-induced apoptosis. *Oncogene* **32**, 341-351 (2013).
15. W. Zhang, J. Xu, K. Wang, X. J. Tang, J. J. He, miR-139-3p suppresses the invasion and migration properties of breast cancer cells by targeting RAB1A. *Oncology Reports* **42**, 1699-1708 (2019).
16. D. H. Ma *et al.*, Baicalein Induces Apoptosis of Pancreatic Cancer Cells by Regulating the Expression of miR-139-3p and miR-196b-5p. *Front Oncol* **11** (2021).
17. R. Suzuki *et al.*, miR-182 and miR-183 Promote Cell Proliferation and Invasion by Targeting FOXO1 in Mesothelioma. *Front Oncol* **8** (2018).
18. S. Dambal, M. Shah, B. Mihelich, L. Nonn, The microRNA-183 cluster: the family that plays together stays together. *Nucleic Acids Research* **43**, 7173-7188 (2015).
19. H. Yan *et al.*, Upregulation of miR-183-5p is responsible for the promotion of apoptosis and inhibition of the epithelial-mesenchymal transition, proliferation, invasion and migration of human endometrial cancer cells by downregulating Ezrin. *Int J Mol Med* **42**, 2469-2480 (2018).

20. S. T. Hashimi *et al.*, MicroRNA profiling identifies miR-34a and miR-21 and their target genes JAG1 and WNT1 in the coordinate regulation of dendritic cell differentiation. *Blood* **114**, 404-414 (2009).
21. B. B. Dai *et al.*, The Cell Type-Specific Functions of miR-21 in Cardiovascular Diseases. *Front Genet* **11** (2020).
22. M. Drobna *et al.*, hsa-miR-20b-5p and hsa-miR-363-3p Affect Expression of PTEN and BIM Tumor Suppressor Genes and Modulate Survival of T-ALL Cells In Vitro. *Cells-Basel* **9** (2020).
23. Q. Sun *et al.*, Dysregulated miR-363 affects head and neck cancer invasion and metastasis by targeting podoplanin. *Int J Biochem Cell B* **45**, 513-520 (2013).
24. C. Z. Zhang *et al.*, MiR-221 and miR-222 target PUMA to induce cell survival in glioblastoma. *Molecular Cancer* **9** (2010).
25. Y. K. Liang *et al.*, MiR-221/222 promote epithelial-mesenchymal transition by targeting Notch3 in breast cancer cell lines. *Npj Breast Cancer* **4** (2018).
26. J. Y. Wang *et al.*, MiR-29a: a potential therapeutic target and promising biomarker in tumors. *Bioscience Rep* **38** (2018).
27. Z. J. Chen *et al.*, miR-342-3p Regulates the Proliferation and Apoptosis of NSCLC Cells by Targeting BCL-2. *Technol Cancer Res T* **20** (2021).
28. X. H. Han *et al.*, MiR-342-3p inhibition promotes cell proliferation and invasion by directly targeting ID4 in pre-eclampsia. *J Obstet Gynaecol Re* **46**, 49-57 (2020).
29. Y. W. Han *et al.*, miR-342-3p promotes osteogenic differentiation via targeting ATF3. *Febs Letters* **592**, 4051-4065 (2018).
30. A. Sharma *et al.*, Posttranscriptional regulation of interleukin-10 expression by hsa-miR-106a. *P Natl Acad Sci USA* **106**, 5761-5766 (2009).
31. Y. Yang *et al.*, MicroRNA-218 functions as a tumor suppressor in lung cancer by targeting IL-6/STAT3 and negatively correlates with poor prognosis. *Molecular Cancer* **16** (2017).
32. S. Z. Liu *et al.*, The miR-106b/NR2F2-AS1/PLEKHO2 Axis Regulates Migration and Invasion of Colorectal Cancer through the MAPK Pathway. *Int J Mol Sci* **22** (2021).
33. J. R. Dobson *et al.*, hsa-mir-30c promotes the invasive phenotype of metastatic breast cancer cells by targeting NOV/CCN3. *Cancer Cell International* **14** (2014).
34. S. Wang *et al.*, Hsa-miR-24-3p increases nasopharyngeal carcinoma radiosensitivity by targeting both the 3'UTR and 5'UTR of Jab1/CSN5. *Oncogene* **35**, 6096-6108 (2016).
35. A. Soriano-Arroquia *et al.*, miR-24 and its target gene Prdx6 regulate viability and senescence of myogenic progenitors during aging. *Aging Cell* **20** (2021).
36. L. Yan *et al.*, miR-24-3p promotes cell migration and proliferation in lung cancer by targeting SOX7. *J Cell Biochem* **119**, 3989-3998 (2018).